Journal of the Korean Physical Society, Vol. 43, No. 2, August 2003, pp. 193∼201

Global Effect of Transverse Bifurcations in Coupled Chaotic Systems

Woochang LIM* and Sang-Yoon KIM†
Department of Physics, Kangwon National University, Chunchon 200-701

(Received 27 January 2003)

We investigate the global effect of transverse bifurcations in symmetrically coupled one-dimensional maps. A transition from strong to weak synchronization occurs via a first transverse bifurcation of a periodic saddle embedded in a synchronous chaotic attractor (SCA). For the case of a supercritical transverse bifurcation, a soft bubbling transition occurs. On the other hand, a subcritical transverse bifurcation leads to a hard transition. The global effect of such subcritical hard bifurcations are found to depend on whether they may or may not induce a "contact" between the SCA and its basin boundary. For the case of a "contact" bifurcation, an absorbing area, surrounding the SCA and acting as a bounded trapping vessel, disappears; hence, basin riddling occurs. However, for the case of a "non-contact" bifurcation, such an absorbing area is preserved; hence, hard bubbling takes place. Through a detailed numerical analysis, we give explicit examples for all kinds of transverse bifurcations leading to bubbling and riddling.

PACS numbers: 05.45.Xt
Keywords: Chaos synchronization, Transverse bifurcation

I. INTRODUCTION

Recently, the phenomenon of synchronization in coupled chaotic systems has become a field of intensive research. When identical chaotic systems synchronize, a chaotic motion occurs on an invariant subspace of the whole phase space [1–4]. Particularly, this type of chaos synchronization has attracted much attention because of its potential practical applications (*e.g.*, see Ref. 5).

An important problem in this field concerns stability of chaos synchronization with respect to a perturbation transverse to the invariant subspace [6]. If a synchronous chaotic state on the invariant subspace is transversely stable, then it may become an attractor in the whole phase space. The properties of the transverse stability of a synchronous chaotic attractor (SCA) are intimately associated with transverse bifurcations of periodic saddles embedded in the SCA [7–13]. If all such periodic saddles are transversely stable, then the SCA becomes asymptotically stable (*i.e.*, Lyapunov stable and attracting in the topological sense); hence, we have "strong" synchronization. However, as the coupling parameter passes through a threshold value, a periodic saddle first becomes transversely unstable through a local bifurcation. After this first transverse bifurcation, trajectories may be locally repelled from the invariant subspace when they visit the neighborhood of the transversely unstable periodic repeller. Thus, loss of strong synchronization begins with such a first transverse bifurcation of an embedded periodic saddle; then, we have "weak" synchronization.

However, the fate of locally repelled trajectories through the first transverse bifurcation depends on whether there exists an absorbing area, controlling the global dynamics, inside the basin of attraction [10–14]. If there exists an absorbing area, surrounding the SCA and acting as a bounded trapping vessel, locally repelled trajectories are restricted to move within the absorbing area and exhibit intermittent bursting from the invariant subspace. For this case, the SCA is transversely stable because its transverse Lyapunov exponent is negative. Hence, the burst will tend to stop. However, in a real situation, a small parameter mismatch or noise results in a continual sequence of intermittent bursts, called attractor bubbling [15–17]. Thus, in the presence of an absorbing area, a bubbling transition occurs through the first transverse bifurcation. For a soft bubbling transition, the maximum bursting amplitude increases gradually from zero with increasing coupling parameter, while for a hard bubbling transition the bursts appear abruptly with large amplitude [16]. However, if such an absorbing area does not exist, the locally repelled trajectories will go to another attractor (or infinity). Consequently, the basin of attraction becomes riddled with a dense set of "holes" belonging to the basin of another attractor (or infinity) [18]. Thus, in the absence of an absorbing area, a riddling transition takes place via the first transverse bifurcation. Furthermore, in the presence of parameter mismatch or noise, the SCA with a riddled basin is transformed into a chaotic transient with a finite lifetime [16]. Note that the weakly stable SCA exhibiting bub-

*E-mail: wclim@kwnu.kangwon.ac.kr
†E-mail: sykim@kangwon.ac.kr

bling or riddling is sensitive to parameter mismatch and noise. Recently, we characterized such parameter and noise sensitivity by introducing new quantifiers, called the parameter and noise sensitivity exponents [19].

For the study of chaos synchronization, two coupled identical one-dimensional (1D) logistic maps, exhibiting period doublings, are often used as a model [9–13]. Both the symmetric [9–11] and the asymmetric [12, 13] coupling cases have been considered. In this paper, we investigate the global effect of the first transverse bifurcations in two symmetrically coupled 1D maps. In Sec. II. 1, we first introduce two symmetrically coupled 1D maps and discuss the overall transverse stability of the SCA based on a phase diagram obtained through a detailed numerical analysis. Then, we investigate the global effect of the first transverse bifurcation of an embedded periodic saddle through which a transition from strong to weak synchronization occurs. For the case of a supercritical transverse bifurcation, the unstable manifold of an asynchronous saddle born via the supercritical bifurcation forms an absorbing area within which locally repelled trajectories from the diagonal are restricted. Hence, a supercritical transverse bifurcation leads to soft bubbling [10], as discussed in Sec. II. 2. On the other hand, for the case of a subcritical transverse bifurcation, a hard transition occurs [10]. In order to see the global effect of the subcritical hard bifurcation, we try to find a simple criterion for determination of whether or not an absorbing area is preserved via the subcritical transverse bifurcation.

Two kinds of subcritical transverse bifurcations are thus found, depending on where the asynchronous repeller (with two unstable directions) that causes transverse instability of a synchronous saddle lies. For the first case, such an asynchronous repeller lies at the basin boundary of the SCA. The unstable manifold of the asynchronous repeller forms an absorbing area surrounding the SCA. When a control parameter passes a threshold value, a synchronous saddle becomes transversely unstable by absorbing the asynchronous repeller lying at the basin boundary. Then, the SCA makes contact with its basin boundary at the point(s) of the synchronous saddle, and the absorbing area disappears. Hence, a riddling transition occurs. Hereafter, these bifurcations will be referred to as subcritical "contact" bifurcations. For the second case, an asynchronous repeller, associated with the transverse destabilization of the synchronous saddle, lies strictly inside an absorbing area, in contrast to the first case. As a control parameter passes a threshold value, a synchronous saddle loses its transverse stability through absorption of the asynchronous repeller lying inside the absorbing area. For this case, the original absorbing area with a finite transverse width is preserved because there is no contact between the SCA and its basin boundary. Hence, a hard bubbling transition takes place. Hereafter, these bifurcations will be called subcritical "non-contact" bifurcations. Using this simple "contact" criterion, we investigate the global effect of the subcritical transverse bifurcations in Sec. II. 3. Finally, a summary is given in Sec. III.

II. GLOBAL EFFECT OF THE FIRST TRANSVERSE BIFURCATIONS

We first introduce two symmetrically coupled 1D maps and discuss the overall transverse stability of the SCA based on the phase diagram for chaos synchronization in Sec. II. 1. Then, the global effect of the first transverse bifurcations leading to a transition from strong to weak synchronization is investigated. A supercritical transverse bifurcation leads to soft bubbling. On the other hand, through a subcritical transverse bifurcation, a hard transition occurs. Here, we present a simple contact criterion to determine the global effect of such subcritical hard bifurcations. For the case of a contact bifurcation, a riddling transition occurs while for the case of a non-contact bifurcation, a hard bubbling transition takes place. With explicit examples, we investigate the global effect of the supercritical and the subcritical transverse bifurcations in Secs. II. 2 and II. 3, respectively.

1. Transverse Stability of the SCA

We consider two symmetrically coupled identical 1D maps T,

$$T : \begin{cases} x_{t+1} = f(x_t) + c\,(y_t - x_t), \\ y_{t+1} = f(y_t) + c\,(x_t - y_t), \end{cases} \tag{1}$$

where x_t and y_t are state variables of the subsystems at a discrete time t, the uncoupled dynamics ($c = 0$) in each subsystem is governed by the 1D map $f(x) = 1 - ax^2$, a is the control parameter of the 1D map, and c is a coupling parameter. This coupled map T has an exchange symmetry because it is invariant under the exchange of coordinates $x \leftrightarrow y$. The set of points which are invariant under the exchange operation forms an invariant symmetry line $y = x$. If an orbit lies on the invariant line, it is called a synchronous orbit because the two state variables x_t and y_t become same for all t; otherwise, it is called an asynchronous orbit.

We also note that the coupled map T is non-invertible because its Jacobian determinant $\det(DT)$ (DT is the Jacobian matrix of T) becomes zero along the critical curve $L_0 = \{(x, y) \in R^2 : (2ax + c)(2ay + c) - c^2 = 0\}$. Critical curves of rank k, L_k ($k = 1, 2, \ldots$), are then given by the images of L_0 [*i.e.*, $L_k = T^k(L_0)$]. Segments of these critical curves can be used to bound a compact region of the phase space that acts as a trapping bounded vessel, called an absorbing area $\mathcal{A}$, inside which trajectories starting near the diagonal are confined [14]. Furthermore, the boundary of an absorbing area can be obtained by the union of segments of the critical curves

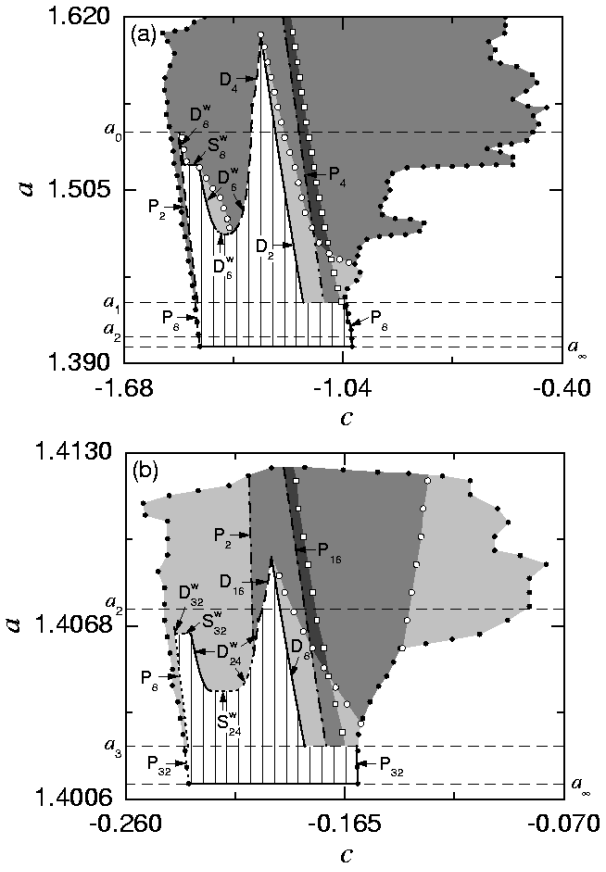

Fig. 1. Phase diagrams for (a) the first and (b) the second largest regions of chaos synchronization in symmetrically coupled 1D maps. The SCA appears when crossing the critical lines denoted by the horizontal solid lines on the $a = a_\infty$ line. Note that the SCA is strongly stable in the hatched region with vertical lines. The non-horizontal boundary curves D_q and P_q of the hatched region correspond to the first transverse period-doubling and pitchfork bifurcation curves of saddles with period q embedded in the SCA, respectively. The boundary curves D_6^w and D_4 in (a) [D_{24}^w and D_{16} in (b)] connect at a point denoted by a small solid circle. On the other hand, the horizontal boundary curve S_q represents the synchronous saddle-node bifurcation opening a periodic window. Here, the superscript "w" in S_q or D_q denotes that the bifurcation is associated with a periodic window. When passing a solid or a dotted part of the boundary, a bubbling transition occurs while a riddling transition takes place when passing a dashed part. Such bubbling and riddling regions are shown in light gray and gray, respectively. Finally, the weakly stable SCA becomes transversely unstable via a blowout bifurcation when passing the boundary curve denoted by solid circles. For more detail, see the text.

and portions of the unstable manifold of an unstable periodic orbit. For this case, $\mathcal{A}$ is called a mixed absorbing area.

With increasing control parameter a, the coupled map T exhibits an infinite sequence of period-doubling bifurcations of synchronous attractors with period 2^n ($n = 0, 1, 2, \ldots$), ending at the accumulation point a_∞ ($= 1.401\,155\cdots$) in some region of c. When crossing a critical line in the $a - c$ plane, a transition from periodic to chaotic synchronization occurs. Figures 1(a) and 1(b) show the phase diagrams for the first and the second largest synchronization regions, respectively. The SCA appears when crossing the critical lines, denoted by the horizontal solid lines on the $a = a_\infty$ line. With further increases of a from a_∞, a sequence of band-merging bifurcations of the SCA takes place. For $a = a_n$, the 2^{n+1} bands of the SCA merge into the 2^n bands; the $a = a_0$ ($= 1.543\,689\ldots$), $a = a_1$ ($= 1.430\,357\cdots$), $a = a_2$ ($= 1.407\,405\cdots$), and $a = a_3$ ($= 1.402\,492\cdots$) lines are shown in the figures.

For the chaotic values of a, the SCA is at least weakly stable inside the region bounded by the solid circles in Figs. 1(a) and 1(b) because its transverse Lyapunov exponent

$$\sigma_\perp = \lim_{N\to\infty} \frac{1}{N} \sum_{t=1}^{N} \ln |2ax_t + 2c| \tag{2}$$

is negative. We note that the SCA becomes strongly stable in the hatched region with vertical lines because there all periodic saddles embedded in the SCA are transversely stable. When crossing the boundary of this hatched region, a transition from strong to weak synchronization occurs. The non-horizontal boundary curves D_q and P_q of the hatched region represent the first transverse period-doubling (PD) and pitchfork (PF) bifurcations of an embedded saddle with period q, which occur when the transverse Floquet (stability) multiplier,

$$\lambda_\perp = \prod_{t=1}^{q} (-2ax_t - 2c), \tag{3}$$

passes through -1 and $+1$, respectively. These transverse PD and PF bifurcations may be supercritical or subcritical. The solid curves denote supercritical transverse bifurcations while the dashed and the dotted curves represent subcritical transverse bifurcations. When crossing a supercritical curve, a soft bubbling transition occurs. However, a hard transition takes place when passing a subcritical curve. The global effect of subcritical hard bifurcations is found to depend on whether they may or may not induce a contact between the SCA and its basin boundary. When crossing a contact bifurcation curve, denoted by a dashed line, a riddling transition occurs. On the other hand, a hard bubbling transition takes place when crossing a non-contact bifurcation curve, denoted by a dotted line. Besides these transverse bifurcation curves, a horizontal boundary curve S_q, representing a synchronous saddle-node bifurcation through which a periodic window opens, exists. When crossing a dotted or dashed part of this horizontal boundary curve, a hard bubbling or riddling transition occurs, respectively. In the phase diagrams, the bubbling and the riddling regions are shown in light gray and gray, respectively. For the bubbling case, an absorbing area, restraining bursting from the diagonal, exists.

However, in the riddling case, no such an absorbing area exists; hence, the basin of the SCA becomes riddled with a dense set of holes belonging to the basin of another attractor (or infinity).

In the region of weak synchronization, two types of transitions from bubbling to riddling occur. When an absorbing area makes contact with the basin boundary, it breaks up; then, a dense set of holes, leading to divergent orbits, fills the basin of the SCA [10]. This boundary crisis of the absorbing area occurs when passing the curve denoted by open circles. Such a transition from bubbling to riddling may also occur via stabilization of an asynchronous saddle inside the absorbing area [9]. Then, the basin of the SCA is riddled with a dense set of holes belonging to the basin of the asynchronous attractor stabilized via a subcritical pitchfork bifurcation. This kind of basin riddling takes place when crossing a dash-dotted curve. Thus, in the dark gray region, the basin of the SCA becomes riddled with two dense sets of holes belonging to the basin of the attractor at infinity and to the basin of an asynchronous attractor inside the absorbing area. Note also that the asynchronous chaotic attractor developed from the stabilized asynchronous periodic attractor disappears via a boundary crisis when crossing a curve denoted by open squares. Then, a reverse transition from riddling to bubbling occurs. Finally, when crossing the boundary denoted by solid circles, the SCA becomes transversely unstable through a blowout bifurcation [20]; then, a complete desynchronization occurs.

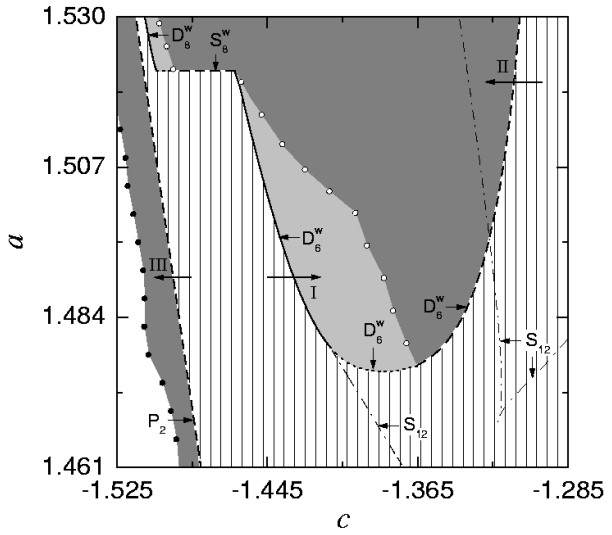

Fig. 2. Magnified phase diagram of Fig. 1(a) near the D_6^w curve. A lower asynchronous period-12 saddle-node bifurcation curve S_{12} (denoted by a dash-dotted line) touches the PD bifurcation curve D_6^w and decomposes it into the supercritical solid and the subcritical dashed and the dotted parts. Furthermore, the boundary crisis curve of an absorbing area (denoted by open circles) crosses the D_6^w curve and decomposes the subcritical part into the dashed contact and dotted noncontact subparts. A pair of asycnhronous period-12 saddle-node bifurcation curves S_{12} (denoted by a dash-dotted line) that emanates from a cusp is associated with the subcritical contact bifurcation occurring when crossing the dashed part of the D_6^w curve. Here, the bubbling and the riddling regions are shown in light gray and gray, respectively. For more detail, see the text.

2. Consequence of Supercritical Transverse Bifurcations

In this subsection, we study the global effect of the first supercritical transverse PD and PF bifurcations that occur when crossing the solid parts of the boundary of the strongly stable region of the SCA in Figs. 1(a) and 1(b). For this case, a soft bubbling transition occurs because the unstable manifold of an asynchronous saddle born via the supercritical transverse bifurcation forms a mixed absorbing area surrounding the SCA.

As an example, we consider the first supercritical PD bifurcation of an embedded period-6 saddle (born via a saddle-node bifurcation) that occurs when crossing the solid part of the D_6^w curve. Figure 2 shows a magnified phase diagram of Fig. 1(a) near the D_6^w curve. Note that a lower asynchronous period-12 saddle-node bifurcation line S_{12}, denoted by a dash-dotted line, touches the D_6^w curve and decomposes it into the supercritical (solid) and subcritical (dashed and dotted) parts. We fix the value of a as $a = 1.49$ and increase the coupling parameter c along route I in Fig. 2. Then, when crossing the solid part of D_6^w for $c = -1.430\,753$, the embedded period-6 saddle (denoted by open circles) becomes transversely unstable via the transverse PD bifurcation, and a new asynchronous saddle with period 12 is born. For this case, the unstable manifold of the newly born asynchronous period-12 saddle (denoted by solid circles) forms a mixed absorbing area surrounding the SCA together with segments of the critical curves, as shown in Fig. 3 for $c = -1.42$. Thus, burstings from the diagonal are restrained within the mixed absorbing area. The "transverse" size of this mixed absorbing area increases gradually from zero because the orbit points of the asynchronous saddle move away continuously from the diagonal. Hence, a soft bubbling transition occurs in the presence of parameter mismatch or noise because the maximum bursting amplitude increases gradually from zero with increasing coupling parameter from the transverse PD bifurcation point. In Fig. 2, such a bubbling region is shown in light gray. We may also enter the bubbling region by passing the dotted part of D_6^w. However, for this case, the synchronous period-6 saddle becomes transversely unstable via a subcritical PD non-contact bifurcation through absorption of an asynchronous repeller with period 12 that is born via a saddle-node bifurcation at the lower dash-dotted line S_{12}. The unstable manifold of an asynchronous period-12 saddle, born at the same lower dash-dotted line S_{12}, forms a mixed absorbing area surrounding the SCA before entering the

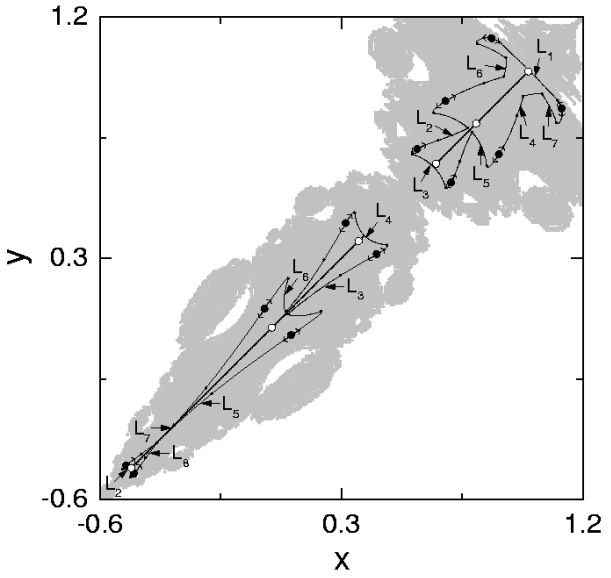

Fig. 3. Symmetric mixed absorbing area surrounding the two-band SCA for $a = 1.49$ and $c = -1.42$ after the supercritical transverse PD bifurcation of a synchronous period-6 saddle (denoted by open circles and embedded in the SCA). The unstable manifold (whose direction is denoted by arrows) of the newly-born asynchronous saddle with period 12 (denoted by solid circles) forms a symmetric mixed absorbing area together with segments of the critical curves L_k $(k = 1, \ldots, 8)$ inside the basin of the SCA (shown in light gray). Here, the dots indicate where the segments of the critical curves and the unstable manifold connect.

bubbling region. Note that this mixed absorbing area is preserved when crossing the dotted part of D_6^w. Hence, a hard bubbling transition occurs. The global effect of this subcritical PD non-contact bifurcation will be discussed in detail in the subsection II. 3. B.

As explained above, a mixed absorbing area surrounds the SCA in the bubbling region (shown in light gray). However, when crossing the boundary curve, denoted by open circles, the absorbing area is destroyed through a boundary crisis. Then, a transition from bubbling to riddling occurs because the basin of the SCA becomes riddled with a dense set of holes, leading to divergent orbits. Such a riddling region is shown in gray.

3. Consequence of Subcritical Transverse Bifurcations

Unlike the case of supercritical transverse bifurcations, a hard transition occurs through a first subcritical transverse bifurcation when crossing a dashed or dotted part of the non-horizontal boundary curve of the hatched region of strong synchronization in Figs. 1(a) and 1(b). The global effect of such subcritical hard bifurcations is found to depend on whether they may or may not induce a contact between the SCA and its basin boundary. A subcritical bifurcation line may be divided into dashed contact and dotted non-contact parts. For the case of a contact bifurcation, an absorbing area surrounding the SCA disappears; hence, basin riddling occurs when crossing a dashed part. On the other hand, for the case of a non-contact bifurcation, such an absorbing area is preserved. As a result, hard bubbling takes place when crossing a dotted part.

A. Subcritical Contact Bifurcations Leading to Riddling

Here, we study the global effect of the first subcritical transverse bifurcations that induce a contact between the SCA and its basin boundary. Such contact bifurcations occur on the dashed part of the non-horizontal boundary curve of the hatched region of strong synchronization. Before a contact bifurcation, the unstable manifold of an asynchronous repeller (with two unstable directions) that lies at the basin boundary forms a mixed absorbing area surrounding the SCA. However, when passing a threshold value, a synchronous saddle becomes transversely unstable by absorbing the asynchronous repeller lying at the basin boundary. Then the SCA makes contact with its basin boundary, and the mixed absorbing area disappears. Consequently, a riddling transition occurs. With explicit examples, the subcritical PD and PF contact bifurcations are discussed in detail below.

As an example, we first consider the subcritical PD contact bifurcation of a synchronous period-6 saddle that occurs when passing the dashed part of the D_6^w curve in Fig. 2. Near this D_6^w curve, a pair of asynchronous period-12 saddle-node bifurcation curves S_{12}, denoted by a dash-dotted line and associated with the subcritical PD bifurcation, emanates from a cusp. We fix the value of a as $a = 1.52$ and decrease the coupling parameter c along route II in Fig. 2. For this case, a asynchronous period-12 saddle and a repeller are born for $c = -1.193\,853$ at the right saddle-node bifurcation curve (emanating from the cusp). Just after the saddle-node bifurcation, the unstable manifold of the asynchronous period-12 saddle forms a mixed absorbing area surrounding the SCA. However, as c is decreased a little more, such an absorbing area breaks up through a boundary crisis for $c \simeq -1.1945$; then, the asynchronous period-12 repeller lies at the basin boundary of the SCA. After that, the "longitudinal" unstable manifold of the asynchronous period-12 repeller (denoted by solid circles) that lies at the basin boundary forms a mixed absorbing area surrounding the SCA, as shown in Fig. 4(a) for $c = -1.3$. As c is further decreased, the asynchronous period-12 saddle disappears via a saddle-node bifurcation for $c = -1.337\,806$ at the left saddle-node bifurcation line (emanating from the cusp). On the other hand, the asynchronous period-12 repeller approaches the synchronous period-6 saddle (denoted by open circles), and the size of the mixed absorbing area shrinks. Eventually, at the subcritical PD bi-

furcation point $c = -1.313\,742$, the synchronous period-6 saddle absorbs the asynchronous period-12 repeller lying at the basin boundary; hence, the mixed absorbing area disappears. Since the SCA touches its basin boundary at the saddle points, the subcritical PD bifurcation induces a contact between the SCA and its basin boundary. After this subcritical PD contact bifurcation, the basin of the SCA becomes riddled with a dense set of holes, leading to divergent trajectories, as shown in Fig. 4(b) for $c = -1.38$. In a real situation, where a small parameter mismatch or noise exists, the SCA with a riddled basin is transformed into a chaotic transient with a finite lifetime.

As a second example, we consider the subcritical PF contact bifurcation of a synchronous period-2 saddle that occurs when crossing the dashed P_2 line in Fig. 2. We fix the value of a as $a = 1.49$ and decrease the coupling parameter c along route III in Fig. 2. As in the above PD case, a pair of asynchronous period-2 repellers (denoted by solid up and down triangles) that lies at the basin boundary approaches the synchronous period-2 saddle (denoted by open circles), and their unstable manifolds form a mixed absorbing area surrounding the SCA, as shown in Fig. 5(a) for $c = -1.48$. As c is decreased, the size of the absorbing area shrinks. Eventually, for $c = -1.494\,987$, the synchronous period-2 saddle becomes transversely unstable via a subcritical PF bifurcation by absorbing the two asynchronous period-2 repellers lying at the basin boundary; then, the absorbing area disappears. Note that this subcritical PF bifurcation also induces a contact between the SCA and its basin boundary. Through this subcritical PF contact bifurcation, basin riddling occurs, as shown in Fig. 5(b) for $c = -1.51$. In the presence of parameter mismatch or noise, the riddled basin SCA is changed into a chaotic transient with a finite lifetime.

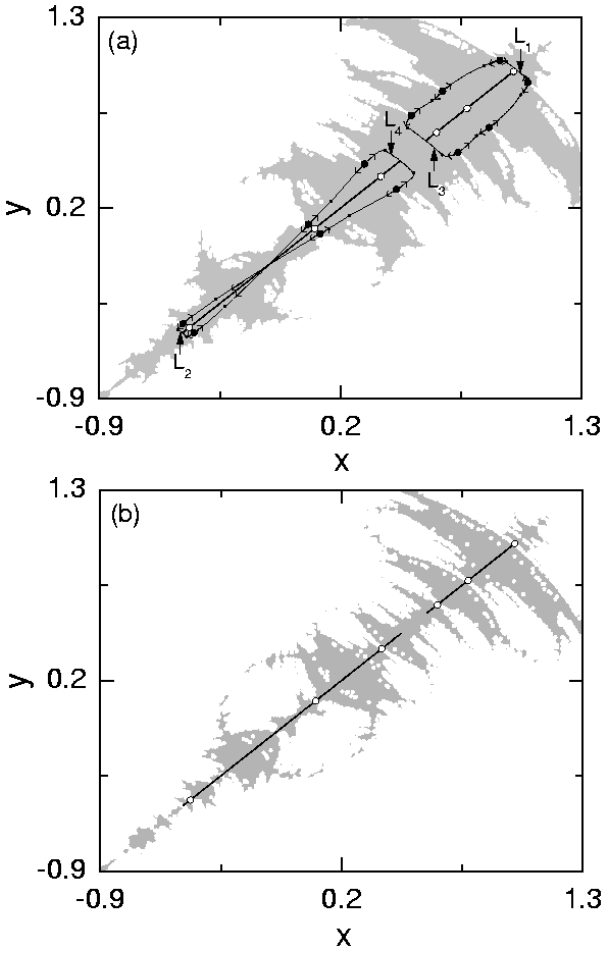

Fig. 4. (a) Symmetric mixed absorbing area surrounding the two-band SCA for $a = 1.52$ and $c = -1.3$ before the subcritical PD contact bifurcation of the synchronous period-6 saddle (denoted by open circles and embedded in the SCA). The unstable manifold (whose direction is denoted by arrows) of the asynchronous period-12 repeller (denoted by solid circles) that lies at the basin boundary forms a symmetric mixed absorbing area together with segments of the critical curves L_k $(k = 1, \ldots, 4)$ inside the basin (shown in light gray) of the SCA. Here, the dots indicate where the segments of the critical curves and the unstable manifold connect. (b) Riddled basin of the SCA for $a = 1.52$ and $c = -1.38$ after the subcritical PD contact bifurcation.

B. Subcritical Non-Contact Bifurcations Leading to Hard Bubbling

We investigate the global effect of the first subcritical non-contact bifurcations. For this case, an asynchronous repeller, causing the transverse instability of a synchronous saddle, lies strictly inside an absorbing area. This is in contrast to the case of contact bifurcations. As a control parameter passes a threshold value, the synchronous saddle loses its transverse stability by absorbing the asynchronous repeller lying inside the absorbing area. However, for this case, the original absorbing area is preserved because there is no contact between the SCA and its basin boundary. As a result, a hard bubbling transition occurs. Explicit examples of the subcritical PD and PF non-contact bifurcations are presented below with a detailed explanation.

As an example, we first consider the subcritical PD non-contact bifurcation of a synchronous period-24 saddle (born via a saddle-node bifurcation) that occurs when crossing the dotted part of the D_{24}^{w} curve in Fig. 1(b). Figure 6 shows a magnified phase diagram of Fig. 1(a) near the D_{24}^{w} curve. An asynchronous period-2 saddle becomes stabilized when crossing the dash-dotted subcritical PF bifurcation line P_2; then, the basin of the SCA becomes riddled with a dense set of holes belonging to the basin of the stabilized asynchronous period-2 attractor. Thus, a transition from bubbling (shown in light gray) to riddling (shown in gray) occurs. Note that this stabilization line P_2 touches the right subcritical part of the D_{24}^{w} curve and decomposes it into the

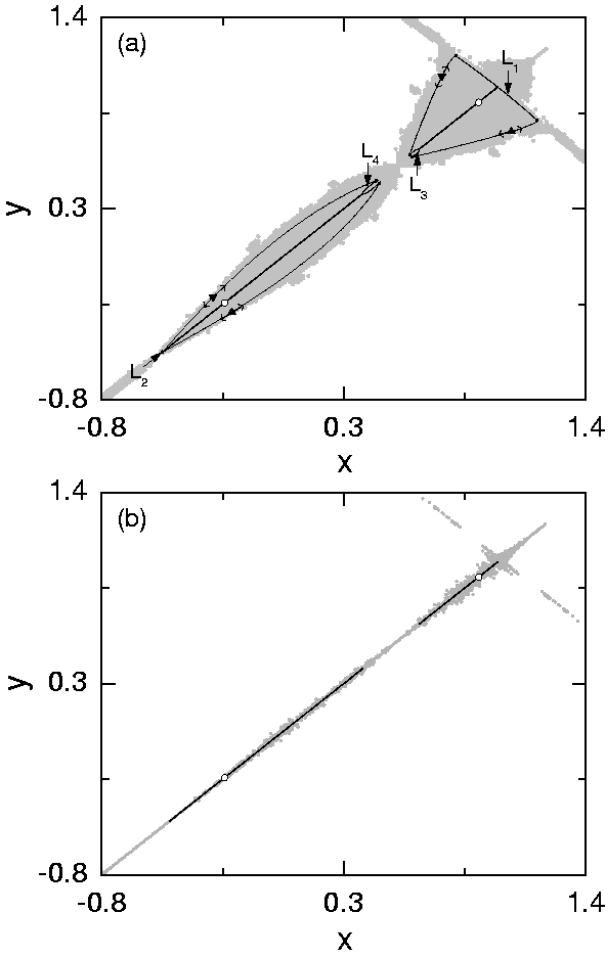

Fig. 5. (a) Symmetric mixed absorbing area surrounding the two-band SCA for $a = 1.49$ and $c = -1.48$ before the subcritical PF contact bifurcation of the synchronous period-2 saddle (denoted by open circles and embedded in the SCA). The unstable manifolds (whose directions are denoted by arrows) of a pair of asynchronous period-2 repellers (denoted by solid up and down triangles) that lies at the basin boundary forms a symmetric mixed absorbing area together with segments of the critical curves L_k $(k = 1, 2)$ inside the basin (shown in light gray) of the SCA. Here, the dots indicate where the segments of the critical curves and the unstable manifold connect. (b) Riddled basin of the SCA for $a = 1.49$ and $c = -1.51$ after the subcritical PF contact bifurcation.

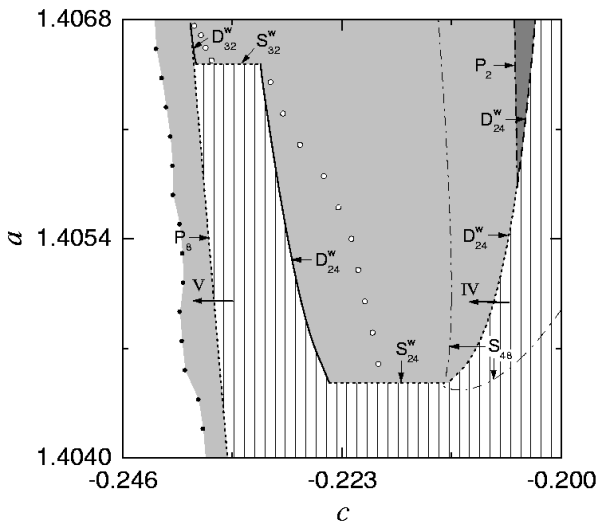

Fig. 6. Magnified phase diagram of Fig. 1(b) near the D_{24}^w curve. An asynchronous period-2 saddle becomes stabilized when crossing the dash-dotted subcritical PF bifurcation line P_2. Then, a transition from bubbling to riddling occurs. Here, the bubbling and the riddling regions are shown in light gray and gray, respectively. Note that this stabilization line P_2 crosses the D_{24}^w curve and decomposes its subcritical part into the dashed contact and the dotted non-contact subparts. A pair of asynchronous period-48 saddle-node bifurcation curves S_{48} (denoted by a dash-dotted line) that emanates from a cusp is associated with the subcritical PD bifurcation occurring when crossing the (dashed and dotted) subcritical part of the D_{24}^w curve. On the other hand, when crossing the solid part of the D_{24}^w curve, a supercritical PD bifurcation occurs. Furthermore, a transition from a small to a large absorbing area occurs through an interior crisis when crossing the curve denoted by open circles. Then, the maximum bursting amplitude increases abruptly. For more detail, see the text.

dashed contact and dotted non-contact subparts. Near this subcritical part of the D_{24}^w curve, a pair of asynchronous period-48 saddle-node bifurcation curves S_{48} (denoted by a dash-dotted curve) emanates from a cusp. We now fix the value of a as $a = 1.405$ and decrease the coupling parameter c along route IV in Fig. 6. Figure 7(a) shows a large absorbing area surrounding the SCA for $c = -0.202$. Note that an asynchronous period-48 repeller (denoted by solid circles) that is born at the right saddle-node bifurcation curve (emanating from the cusp) for $c = -0.199\,438$ lies strictly inside the absorbing area [see Figs. 7(a) and 7(b)]. As c is decreased, this asynchronous period-48 repeller approaches the synchronous period-24 saddle (denoted by open circles). Eventually, when crossing the dotted part of the D_{24}^w curve for $c = -0.207\,085$, the synchronous period-24 saddle becomes transversely unstable via a subcritical PD bifurcation by absorbing the asynchronous period-48 repeller lying inside the absorbing area. For this case, the absorbing area surrounding the SCA is preserved, as shown in Fig. 7(c) for $c = -0.213$, because no contact between the SCA and its basin boundary occurs. This is in contrast to the case of the above contact bifurcations. After this subcritical PD non-contact bifurcation, transient intermittent bursts with large amplitudes appear abruptly [see Fig. 7(d)]. For this case, the maximum bursting amplitude is determined by the transverse size of the absorbing area. In a real situation, a small parameter mismatch or noise leads to a persistent sequence of intermittent bursts. Thus, a hard bubbling transition occurs through the subcritical PD non-contact bifurcation.

As a second example, we consider the subcritical PF non-contact bifurcation that occurs when crossing the

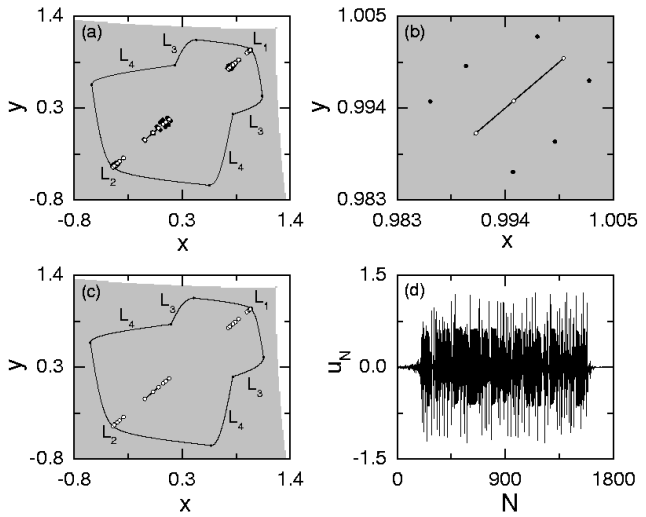

Fig. 7. (a) Large absorbing area surrounding the eight-band SCA for $a = 1.405$ and $c = -0.202$ before the subcritical PD non-contact bifurcation of the synchronous period-24 saddle (denoted by open circles and embedded in the SCA). The absorbing area is bounded by segments of the critical curves L_k $(k = 1, \ldots, 4)$ inside the basin of attraction (shown in light gray). Here the dots indicate where the segments of the critical curves connect. An asynchronous period-48 repeller (denoted by solid circles) lies strictly inside the absorbing area. For a clear view of this asynchronous period-48 repeller, a magnified view of (a) near the topmost band of the SCA is given in (b). For $c = -0.207\,085$, the synchronous period-24 saddle becomes transversely unstable via a subcritical PD non-contact bifurcation by absorbing the asynchronous period-48 repeller. (c) Preserved absorbing area surrounding the SCA for $a = 1.405$ and $c = -0.213$ after the subcritical PD non-contact bifurcation. (d) Transient intermittent bursting for a trajectory starting from an initial point $(x_0, y_0) = (0.12, 0.13)$ when $a = 1.405$ and $c = -0.213$. Here, the transverse variable $u(\equiv y - x)$ represents the deviation from the diagonal.

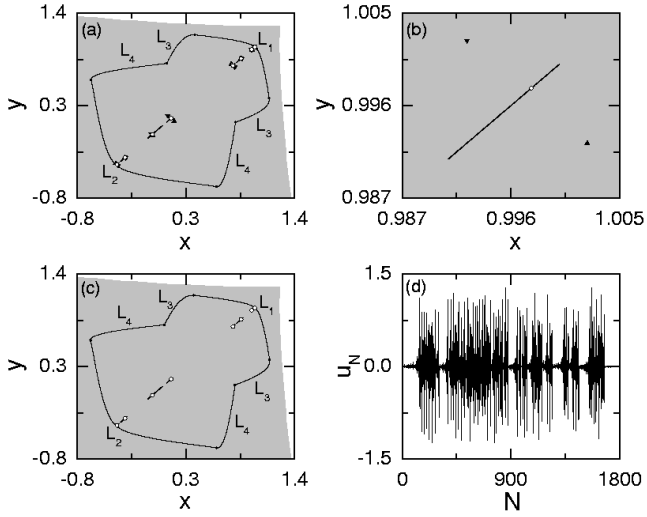

Fig. 8. (a) Large absorbing area surrounding the eight-band SCA for $a = 1.405$ and $c = -0.233$ before the subcritical PF noncontact bifurcation of the synchronous period-8 saddle (denoted by open circles). The absorbing area is bounded by segments of the critical curves L_k $(k = 1, \ldots, 4)$ inside the basin of attraction (shown in light gray). Here, the dots indicate where the segments of the critical curves connect. A pair of asynchronous period-8 repellers (denoted by solid up and down triangles) lies strictly inside the absorbing area. For a clear view of the asynchronous period-8 repellers, a magnified view of (a) near the topmost band of the SCA is given in (b). For $c = -0.236\,431$, the synchronous period-8 saddle becomes transversely unstable via a subcritical PF noncontact bifurcation by absorbing a pair of asynchronous period-8 repellers. (c) Preserved absorbing area surrounding the SCA for $a = 1.405$ and $c = -0.239$ after the subcritical PD non-contact bifurcation. (d) Transient intermittent bursting for a trajectory starting from an initial point $(x_0, y_0) = (0.9, 0.91)$ when $a = 1.405$ and $c = -0.239$. Here, the transverse variable $u(\equiv y - x)$ represents the deviation from the diagonal.

dotted P_8 line in Fig. 6. We fix the value of a as $a = 1.405$ and decrease the coupling parameter along route V in Fig. 6. A pair of asynchronous period-8 repellers (denoted by solid up and down triangles) lies strictly inside the large absorbing area, as shown in Figs. 8(a) and 8(b) for $c = -0.233$. As c is decreased, they approach the synchronous period-8 saddle (denoted by open circles). Eventually, for $c = -0.236\,431$, the synchronous period-8 saddle loses its transverse stability via a subcritical PF bifurcation by absorbing the asynchronous period-8 repellers. Note that the large absorbing area is preserved because this subcritical PF bifurcation induces no contact between the SCA and its basin boundary [see Fig. 8(c)]. Then, as shown in Fig. 8(d) for $c = -0.239$, a sequence of transient intermittent bursts with large amplitudes appears abruptly. Thus, in the presence of a small parameter mismatch or noise, a hard bubbling transition takes place via the subcritical PF non-contact bifurcation.

III. SUMMARY

We have investigated the global effect of the first transverse bifurcations in symmetrically coupled 1D maps. Through a detailed numerical analysis, we have given explicit examples for the consequence of supercritical and subcritical transverse bifurcations. For the supercritical case, soft bubbling transition occurs, while a hard transition takes place for the subcritical case. For the determination of the global effect of subcritical hard bifurcations, a simple contact criterion has been presented. For the case of a subcritical contact bifurcation, an absorbing area that exists before the bifurcation disappears because the SCA makes contact with its basin boundary; hence, basin riddling occurs. However, for the case of a subcritical non-contact bifurcation, the original absorbing area surrounding the SCA is preserved because no contact between the SCA and its basin boundary occurs. Consequently, a hard bubbling transition takes place.

ACKNOWLEDGMENTS

This work was supported by the Korea Research Foundation (Grant No. KRF-2001-013-D00014).

REFERENCES

[1] H. Fujisaka and T. Yamada, Prog. Theor. Phys. **69**, 32 (1983).
[2] A. S. Pikovsky, Z. Phys. B: Condens. Matter **50**, 149 (1984).
[3] V. S. Afraimovich, N. N. Verichev and M. I. Rabinovich, Radiophys. Quantum Electron. **29**, 795 (1986).
[4] L. M. Pecora and T. L. Carroll, Phys. Rev. Lett. **64**, 821 (1990).
[5] K. M. Cuomo and A. V. Oppenheim, Phys. Rev. Lett. **71**, 65 (1993); L. Kocarev, K. S. Halle, K. Eckert, L. O. Chua and U. Parlitz, Int. J. Bifurcation Chaos Appl. Sci. Eng. **2**, 973 (1992); L. Kocarev and U. Parlitz, Phys. Rev. Lett. **74**, 5028 (1995); N. F. Rulkov, Chaos **6**, 262 (1996).
[6] P. Ashwin, J. Buescu and I. Stewart, Nonlinearity **9**, 703 (1996).
[7] B. R. Hunt and E. Ott, Phys. Rev. Lett. **76**, 2254 (1996); Phys. Rev. E **54**, 328 (1996).
[8] Y.-C. Lai, C. Grebogi, J. A. Yorke and S. C. Venkataramani, Phys. Rev. Lett. **77**, 55 (1996).
[9] V. Astakhov, A. Shabunin, T. Kapitaniak and V. Anishchenko, Phys. Rev. Lett. **79**, 1014 (1997).
[10] Yu. L. Maistrenko, V. L. Maistrenko, A. Popovich and E. Mosekilde, Phys. Rev. E **57**, 2713 (1998); **60**, 2817 (1999).
[11] Yu. L. Maistrenko, V. L. Maistrenko, A. Popovich and E. Mosekilde, Phys. Rev. Lett. **80**, 1638 (1998); G.-I. Bischi and L. Gardini, Phys. Rev. E **58**, 5710 (1998).
[12] O. Popovych, Yu. L. Maistrenko, E. Moskilde, A. Pikovsky and J. Kurths, Phys. Lett. A **275**, 401 (2000); Phys. Rev. E **63**, 036201 (2001).
[13] S.-Y. Kim and W. Lim, Phys. Rev. E **63**, 026217 (2001); S.-Y. Kim, W. Lim and Y. Kim, Prog. Theor. Phys. **105**, 187 (2001); S.-Y. Kim and W. Lim, Phys. Rev. E **64**, 016211 (2001); W. Lim, S.-Y. Kim and Y. Kim, J. Korean Phys. Soc. **38**, 532 (2001).
[14] C. Mira, L. Gardini, A. Barugola and J.-C. Cathala, *Chaotic Dynamics in Two-Dimensional Noninvertible Maps* (World Scientific, Singapore, 1996); R. H. Abraham, L. Gardini and C. Mira, *Chaos in Discrete Dynamical Systems* (Springer, New York, 1997).
[15] P. Ashwin, J. Buescu and I. Stewart, Phys. Lett. A **193**, 126 (1994); J. F. Heagy, T. L. Carroll and L. M. Pecora, Phys. Rev. E **52**, 1253 (1995).
[16] S. C. Venkataramani, B. R. Hunt, E. Ott, D. J. Gauthier and J. C. Bienfang, Phys. Rev. Lett. **77**, 5361 (1996); S. C. Venkataramani, B. R. Hunt and E. Ott, Phys. Rev. E **54**, 1346 (1996).
[17] J.-H. Cho, D.-U. Hwang, C.-M. Kim and Y.-J. Park, J. Korean Phys. Soc. **39**, 378 (2001).
[18] J. C. Alexander, J. A. Yorke, Z. You and I. Kan, Int. J. Bifurcation Chaos Appl. Sci. Eng. **2**, 795 (1992); E. Ott, J. C. Sommerer, J. C. Alexander, I. Kan and J. A. Yorke, Phys. Rev. Lett. **71**, 4134 (1993); J. C. Sommerer and E. Ott, Nature (London) **365**, 136 (1993); E. Ott, J. C. Alexander, I. Kan, J. C. Sommerer and J. A. Yorke, Physica D **76**, 384 (1994); J. F. Heagy, T. L. Carroll and L. M. Pecora, Phys. Rev. Lett. **73**, 3528 (1994).
[19] A. Jalnine and S.-Y. Kim, Phys. Rev. E **65**, 026210 (2002); S.-Y. Kim, W. Lim, A. Jalnine and S. P. Kuznetsov, Phys. Rev. E **67**, 016217 (2003).
[20] E. Ott and J. C. Sommerer, Phys. Lett. A **188**, 39 (1994); Y. Nagai and Y.-C. Lai, Phys. Rev. E **56**, 4031 (1997).